SLAC – PUB – 3862
SLAC – AP – 45
January 1986
(A/AP)

BELLOWS WAKE FIELDS AND TRANSVERSE SINGLE BUNCH INSTABILITIES IN THE SSC*

K. L. F. BANE AND R. D. RUTH

Stanford Linear Accelerator Center
Stanford University, Stanford, California, 94305

Presented at the SSC Impedance Workshop
Berkeley, California, June 26-27, 1985

⋆ Work supported by the Department of Energy, contract DE-AC03-76SF00515

1. Introduction

In this paper we study the transverse wake field due to the bellows in the SSC and its effect on the transverse mode coupling instability. For long bunches this instability has a small growth rate which depends critically on the real part of the transverse impedance at $\omega \leq 1/\sigma_\tau$ where σ_τ is the bunchlength in seconds. The instability is caused by the coupling of mode 0, the rigid dipole mode, and mode '-1' , the mode shifted by $-\nu_s$ from the betatron tune. Thus, the instability needs a large frequency shift as well as a large 'off diagonal' element to couple the modes. The frequency shift is induced by the imaginary part of the transverse impedance at $\omega \leq 1/\sigma_\tau$ while the off diagonal element is related to the real part of the impedance at $\omega \simeq 1/\sigma_\tau$. In addition, if the beam current is large enough, there can be a coasting-beam-like instability with a growth rate larger than the synchrotron frequency. By comparing the transverse and longitudinal instability thresholds, it is straightforward to see that the single bunch transverse instability is more restrictive than the single bunch longitudinal instability in the SSC.[1]

There have been calculations which suggest that bellows can be a large source of transverse impedance, and thus can drive transverse instabilities.[2,3] Therefore, in this paper we will emphasize the bellows impedance but also include the beam position monitor impedance. There are certainly other sources of transverse impedance which will be omitted here.

In the following sections we first discuss the instability thresholds and then show calculations of the bellows wake fields. To reduce the wake field effects, another design with shielded bellows is then considered. Next we discuss briefly the impedance of the beam position monitors. Finally, we show the effect of the bellows and beam position monitors on transverse mode coupling.

2. Thresholds for Transverse Instabilities

There are two 'types' of transverse instabilities considered here. The first is the transverse mode coupling instability in which two low-order modes couple to cause an instability. The second is the 'transverse microwave' instability which is the coasting-beam-like instability mentioned above. The second of these involves the cooperation of an infinity of the so called head-tail modes and is better analyzed with different techniques.[4,5] It is important to note that in essence these two 'types' of transverse instabilities involve the same physics. The division is made for the purposes of calculation only.

2.1 Threshold for Fast Blow-up [$\Im m(\omega) \gg \omega_s$]

Consider an impedance which is somewhat broad band and large in the neighborhood of some frequency ω_r. The impedance should vary slowly in a frequency range of $1/\sigma_T$. Then the *sufficient condition for no fast blow-up* for a Gaussian bunch is given by[4,5]

$$\frac{eI \mid Z_\perp(\omega_r) \mid \beta_{ave}}{4E\eta\sigma_\epsilon\sigma_T\omega_r} \leq 1 \quad , \tag{1}$$

where

$$\begin{aligned} \sigma_\epsilon &= \Delta p/p \text{ rms} \\ I &= \text{bunch current} \\ E &= \text{energy} \\ \eta &= \text{frequency slip factor} \\ Z_\perp &= \text{transverse impedance} \\ \beta_{ave} &= \text{average beta function} \quad . \end{aligned}$$

The chromaticity is assumed to be zero so that the spread in frequency above is entirely due to the spread in revolution frequency.

Equation (1) can be thought of as the 'threshold' for fast blow-up; however, since it is actually a sufficient condition for *no* fast blow-up, it may be somewhat pessimistic. That is, the actual instability may occur at a current as much as a factor of 2 or 3 more than the current which satisfies the equality in Eq. (1), but the instability will not occur at lower values. We will use the term threshold to refer to the equality in Eq. (1) while keeping in mind this caveat.

2.2 Threshold for the Transverse Mode Coupling Instability[5,6]

This instability has been seen both in PETRA and PEP and is due to the coupling of low order head-tail modes. To estimate the threshold consider the shift of mode 0. For a Gaussian bunch the shift of the rigid dipole mode for small currents is given by

$$\frac{\Delta\nu}{\nu_s} = \frac{-ieI\beta_{ave}}{4\pi E\nu_s} \int_{-\infty}^{\infty} Z_{\perp}(p\omega_0) e^{-p^2\omega_0^2\sigma_\tau^2} dp \quad . \tag{2}$$

If we assume that there is sufficient resistive impedance at $\omega < 1/\sigma_\tau$ to couple modes 0 and -1, then the threshold typically occurs when mode 0 has shifted by about ν_s. For long bunches, however, mode -1 moves down also with a slope which is 1/4 of the slope for mode 0. Thus, a simple extrapolation would yield mode coupling if mode 0 is shifted by about $4\nu_s/3$. This yields a formula for the threshold,

$$\frac{4}{3} \simeq \frac{ieI\beta_{ave}}{4\pi E\nu_s} \int_{-\infty}^{\infty} Z_{\perp}(p\omega_0) e^{-p^2\omega_0^2\sigma_\tau^2} dp \quad . \tag{3}$$

If the bunch is sufficiently long, and the imaginary part of the transverse impedance varies little from 0 to about $1/\sigma_\tau$, the threshold is given approximately by

$$\frac{4}{3} \simeq \frac{eI\Im m[Z_\perp(1/\sigma_\tau)]\beta_{ave}}{4\pi E\nu_s} \frac{\sqrt{\pi}}{\sigma_\tau\omega_0} \quad . \tag{4}$$

If we compare the two thresholds and note that $\nu_s\sigma_\tau\omega_0 = \eta\sigma_\epsilon$, we find

$$\frac{I_{th}(\text{Fast Blow Up})}{I_{th}(\text{Mode Coupling})} = \frac{3\sigma_\tau\omega_r}{4\sqrt{\pi}} \frac{\Im m[Z_\perp(1/\sigma_\tau)]}{\mid Z_\perp(\omega_r)\mid} \quad . \tag{5}$$

3. Bellows Wake Fields/Impedances

The computer code TBCI[7] can be used to calculate the dipole wake field due to a bellows. Ideally we would like the wake field due to a point charge (the δ-function wake) $W_\perp(t)$, from which we get the transverse impedance $Z_\perp(\omega)$ by

$$iZ_\perp(\omega) = \int_0^\infty W_\perp(t)e^{i\omega t}\,dt \quad . \tag{6}$$

The code, however, solves for the wake field of a smooth finite-length bunch, which we will denote by $\bar{W}_\perp(t)$. $\bar{W}_\perp(t)$ is simply the convolution of $W_\perp(t)$ with the current distribution. If a short enough bunch length is chosen, $\bar{W}_\perp$ is very similar to $W_\perp$. For a Gaussian current distribution with rms bunch length σ_τ, the Fourier transform of the bunch wake $\bar{Z}_\perp(\omega)$ is related to the impedance by

$$\bar{Z}_\perp(\omega) = Z_\perp(\omega)e^{-\omega^2\sigma_\tau^2/2} \quad . \tag{7}$$

Given $\bar{Z}_\perp$, Eq. (7) can be used to find $Z_\perp$.

In practice $Z_\perp$ can be found only up to some limiting frequency due to numerical inaccuracies. One such source of inaccuracy is the finite mesh size used in TBCI to calculate $\bar{W}_\perp$. Another source is the Gaussian driving bunch; for $\omega\sigma_\tau$ large enough the Gaussian factor of Eq. (7) destroys all meaningful information in $\bar{Z}_\perp$. In all examples presented here short driving bunches were used with $c\sigma_\tau$ of 1 or 2 mm. The mesh size was taken to equal $c\sigma_\tau/4$. For this situation meaningful information appears to be limited to $\omega/2\pi \simeq 1/2\sigma_\tau$ which for the cases above is 75 or 150 GHz.

For single bunch instability studies it is only necessary to calculate the wake field over a distance equal to the total design bunch length. Since the SSC rms bunch length is 7 cm, it was deemed sufficient to calculate the wake field out to 20 cm. The resolution due to this limited sampling range is $\Delta f = c/20\,\mathrm{cm} = 1.5$ GHz.

3.1 Simple Bellows

Calculation:

The first example is that of a simple rectangular bellows (See Fig. 1a). The actual bellows used may have rounded corners or be triangular in shape, but the rectangular approximation with appropriately chosen dimensions should give the same basic behavior. For the TBCI calculation we have chosen a beam tube radius $b = 1.65$ cm, a bellows period $p = 0.22$ cm and a depth of corrugation $\Delta = 0.35$ cm. These bellows are directly scaled from the PEP inner bellows. Forty cells were used in the computation. The mesh spacing was 1/10 of a period. Fig. 2 gives $\bar{W}_\perp$ in units of V/pC/cell due to a Gaussian bunch with $c\sigma_\tau = 1.0$ mm, centered at $ct = 0$ and with its head at $ct < 0$. Note that the wake has a maximum value of 5.6 V/pC per cell. By taking the Fast Fourier Transform of $\bar{W}_\perp$ and then using Eq. (7), we get the impedance $Z_\perp$ (See Fig. 2). The units are in kΩ/m/cell.

From the plots we see that the bellows impedance is dominated by what appears to be a damped resonance peaked at 13.5 GHz. The peak is above the first TM1 cut-off of the tube, $f_c = (c/2\pi)(3.83/0.0165\text{m}) \approx 11$ GHz. The peak value of $\Re e(Z_\perp)$ is about 370 Ω/m per cell. If we let the quality factor Q be the resonant frequency divided by the full width at half maximum we get $Q \approx 5$. Note that the ratio of the first peak of $\Re e(Z_\perp)$ to the magnitude of $\Im m(Z_\perp)$ near zero also appears to be about 5. (This is consistant with the isolated resonance picture discussed below.) In addition, a second much weaker peak can be seen at 50 GHz.

The SSC bunch samples the impedance up to $\omega/2\pi \sim 0.7$ GHz since the bunch length is 7 cm. Over this frequency range $\Im m(Z_\perp) = -79$ Ω/m per cell. If 1.2 km of bellows are needed, which corresponds to 550,000 of these cells, then $\Im m(Z_\perp) = -43$ MΩ/m for the entire SSC ring. Although this is a large value, the real part of the impedance over this frequency range is very small.

Discussion and Scaling:

The computer code TRANSVRS[8] can be used to calculate the transverse frequencies of infinitely repeating, rectangular bellows. According to this code the first two dipole modes excited by an ultra-relativistic charge traversing the simple bellows described above are at 12.2 GHz and 47.7 GHz. It is this result that leads us to describe the two peaks of $\Re e(Z_\perp)$ as isolated resonances. The frequencies calculated by the two codes compare reasonably well. Further TBCI computations of this bellows, but with a varied number of cells, show an increase in the fundamental frequency ω_0 with a decrease in the number of cells. For the bellows example described above $\omega_0/2\pi = 18$ GHz when only one cell is used. Therefore, the agreement of the two codes for the resonant frequencies of bellows with very many periods may be even better than is apparent here.

In addition, TRANSVRS was used to calculate the fundamental frequency for rectangular bellows with various dimensions. The results can be summarized by the scaling relation

$$\frac{\omega_0 b}{c} = 1.79 \left(\frac{\Delta}{b}\right)^{-0.55} \quad . \tag{8}$$

The above relation gives the TRANSVRS results to within 5% for $0.05 < \Delta/b < 0.30$ and $0.05 < p/b < 0.20$. The discrepancy is largest for Δ/p small. We know that this scaling cannot be valid for structures with $\Delta/p \ll 1$, since for these structures (assuming p/b is small) $\omega_0 p/c \approx \pi$.[9] Such a structure, however, would make a poor bellows!

Since the bellows impedance is dominated by a single mode, its wake field can be written as[10]

$$W_\perp \approx \frac{2c\, k_{\perp 0}}{b^2 \omega_0} \sin \omega_0 t \, \exp\left(-\frac{\omega_0 t}{2Q_0}\right) \qquad \text{for } t > 0 \quad , \tag{9}$$

where ω_0, $k_{\perp 0}$ and Q_0 are respectively the frequency, the strength factor (or loss factor) and the quality factor of the first dipole mode, and ct is the distance that the test charge is behind the driving charge. From Eq. (6) we see immediately that the strength factor is related to the value of $\Im m(Z_\perp(0))$ by

$$\Im m(Z_\perp(0)) \approx -\frac{2c\, k_{\perp 0}}{b^2 \omega_0^2} \quad , \tag{10}$$

when $1/4Q_0^2$ is small. Furthermore, when $1/Q_0$ is small, we have

$$\hat{W}_\perp \approx -\omega_0 \Im m(Z_\perp(0)) \quad , \tag{11}$$

where $\hat{W}_\perp$ is the maximum of $W_\perp$. Neither $\Im m(Z_\perp(0))$ nor $\hat{W}_\perp$ depend on Q_0 for $1/Q_0$ small.

The value of $\Im m(Z_\perp(0))$ can also be approximated by[11]

$$\Im m(Z_\perp(0)) = -\frac{Z_0 p}{2\pi b^2}\frac{s^2-1}{s^2+1} \quad , \tag{12}$$

where $Z_0 = 377\ \Omega$ is the impedance of free space and $s = 1 + \Delta/b$. With the help of Eqs. (8), (10), (11)and (12) the values of ω_0, $k_{\perp 0}$, $\hat{W}_\perp$ and $\Im m(Z_\perp(0))$ can be approximated for most practical simple bellows. For the above example these relations yield $\omega_0/2\pi = 12.2$ GHz, $k_{\perp 0} = 0.25$ V/pC/cell, $\hat{W}_\perp = 7.1$ V/pC/cell and $\Im m(Z_\perp(0)) = -92\,\Omega$/m/cell. These values compare reasonably well with the Fourier transforms of the TBCI calculations.

<u>The Finite Q:</u>

The TBCI computations assume perfectly conducting walls. Under this assumption any trapped mode would have an infinite Q: there would be no energy loss. For a mode above cut-off, however, energy can leak down the beam tube yielding a resonance peak in $\Re e(Z_\perp)$ with a finite width. We can therefore speak of such a mode as having a finite Q. But as the number of periods in our bellows approaches infinity, we expect the Q of this mode also to approach infinity. For a sufficiently large number of bellows periods

$$Q_0 = \frac{\omega_0 U_0}{P_0} = \frac{\omega_0 p}{v_{g0}} N_p \quad , \tag{13}$$

where U_0, P_0, v_{g0} are respectively the total energy stored in the bellows, the power loss and the group velocity of the mode; p is the period of the structure and N_p is the number of bellows periods. In practice for a very large number of periods, the Q will be limited by the finite resistivity of the metal walls. For copper, at these frequencies, the Q will be limited to a value of some thousands. If the cells differ slightly, the effective Q will also be reduced.

For the bellows above, where the wavelength $2\pi c/\omega_0 = 2.2$ cm $=10p$, one would presumably need some tens of periods for the above approximation to be valid. For this example TRANSVRS calculates $v_{g0} = 0.4c$. Therefore, for forty cells, the above approximation yields $Q_0 = 60$.

The code TBCI, however, yields a result of $Q_0 \approx 5$ for 40 cells, which is approximately the same value it gets when only 20 cells are used in the calculation. Numerical errors caused by the finite mesh size used in the TBCI calculation will contribute to field and frequency inaccuracies and therefore to a resonance widening. We have seen indications that this is the cause of the unexpectedly low value of Q_0 computed by TBCI. Unfortunately, it is difficult to use a mesh which is fine enough to investigate this question further. In any case a real bellows has an effective Q_0 limited by the construction imperfections as discussed above. In the subsequent calculations we will assume the Q_0 given by TBCI.

3.2 SHIELDED BELLOWS

Calculations:

An example of a shielded bellows in the expanded position is shown schematically in Fig. 1b. The wiggles at the top of the figure represent the simple bellows that is being shielded. The shielding cylinders which have a thickness of 2 mm overlap by 11 cm when expanded. For this example we choose a gap g of 10 cm and a depth d of 5.5 mm. In order to reduce the number of mesh points required, the actual calculations are done for the structure shown in Fig. 1c. For a wake field reaching only to 20 cm behind the bunch head, the results for the two configurations are the same: no wave launched by the head of the bunch can travel to point P in Fig. 1b and return to a test particle located 20 cm behind the head.

Fig. 3 gives the wake field calculated by TBCI for a bunch with $c\sigma_\tau = 2$ mm. The first peak has a value of 46.3 V/pC/m per shielded bellows. Note that the wake does not exhibit such a clear resonance as before. The period for such a resonant behavior must be about the time for information from the rest of the cavity to return back to the axis. The resultant low frequency resonance will affect only the multi-bunch beam behavior. The value of $\Im m(Z_\perp(0))$ is -2 kΩ/m per shielding unit. Although $\Re e(Z_\perp)$ is again small at low frequencies, it rises much sooner than in the simple bellows case. We see peaks at 3.3 GHz and 9.8 GHz with values of 1.4 $k\Omega$/m and 1.5 $k\Omega$/m respectively.

The impedance of this shielded bellows should be compared to the number of simple bellows it can shield. Let us assume that each unit shields 30 cm of simple bellows, or 136 periods of the simple bellows presented in the previous section. Then 1.2 km of bellows corresponds to 4000 of these shielding units. For the whole machine $\Im m(Z_\perp(0)) = -8.0$ MΩ/m.

Variations and Scaling:

Running the shielded bellows again (with $c\sigma_\tau = 2$ mm) but with $d = 4$ mm results in the wake field of Fig. 4. The wake field looks very similar to that of the previous example. The first peak has a value of 33.6 V/pC/m. The impedance looks similar, though the strong resonance at 9.8 GHz is missing. $\Im m(Z_\perp(0))$ is

-1.1 kΩ/m.

We see that the value of the first peak of the wake scales almost exactly by the ratios of d used in the two cases, *i.e.* 4.0/5.5= 0.73. To test the scaling with g, we have run with g set to 7 cm and 13 cm. Neither case yields a significant change in the peak of the wake field. Therefore, the peak of the wake field is roughly independent of the gap g as long as it is not too small. In summary, for a shielded bellows the peak of the wake field scales as

$$\hat{W}_\perp = \hat{W}_{\perp 0} \left(\frac{b}{b_0}\right)^{-3} \left(\frac{d}{d_0}\right) \quad , \tag{14}$$

where $W_\perp$ is the wake field per shielding unit. The value of $\Im m(Z_\perp(0))$ also follows this scaling approximately.

Finally, the cell of Fig. 1d was used to model the shielded bellows of Fig. 1b but with the space between the two shielding cylinders perfectly closed by something like a metallic washer at position Q. The depth d was set to 4 mm. In this case 136 small corrugations of the simple bellows are replaced by one larger corrugation. Fig. 5 gives the resultant transverse wake field and impedance. The first peak of $\bar{W}_\perp$ has a value of 32.3 V/pC/m. Although the value of the peak of the wake field is approximately the same as in the previous example, in this case the total area under this peak is much less; thus, the impedance is significantly reduced. The value of $\Im m(Z_\perp)$ at 1.5 GHz is -620Ω/m, about half the value without the washer in place. In addition, the resonance peak near 2 GHz has been eliminated. In fact $\Re e(Z_\perp)$ is essentially zero up to about 4 GHz.

3.3 The Longitudinal Impedance of Bellows

Simple Bellows:

TBCI can also be used to calculate the longitudinal wake field $\bar{W}_{\|}$ of a bunch traversing a bellows, from which we can get the longitudinal impedance $Z_{\|}$ just as in the transverse case. The longitudinal wake was calculated for forty periods of the simple bellows introduced in Section 3.1 for a bunch with $c\sigma_\tau = 1$ mm (See Fig. 6.) As in the transverse case, the longitudinal impedance is dominated by what appears to be a damped resonance. The resonant frequency is at 12.3 GHz, which is above the first TM0 cut-off frequency. A second resonance can be seen at 49 GHz. The computer code KN7C,[12] the longitudinal counterpart of TRANSVRS, yields frequency values of 11.6 GHz and 47.7 GHz for the first two longitudinal modes. It is interesting to note that the first two longitudinal modes are almost at the same frequency as the first two dipole modes.

For the SSC, the heating of the walls is the only effect of the longitudinal wake which we need to consider. Given the total loss factor $k_{\|tot}$, the power lost per turn is given by

$$P = k_{\|tot}\, e^2 N^2 n_b f_{rev} \quad , \tag{15}$$

where N is the number of particles per bunch, n_b is the number of bunches and f_{rev} is the revolution frequency. For a Gaussian bunch $k_{\|tot}$ is given by

$$k_{\|tot} = \frac{1}{\pi} \int_0^\infty \Re e(Z_{\|}) e^{-\omega^2\sigma_\tau^2}\, d\omega \quad . \tag{16}$$

For the simple bellows $\Re e(Z_{\|})$ is so small over the bunch spectrum that $k_{\|tot}$ is completely negligible. For example, at 8 GHz, where $\Re e(Z_{\|})$ begins to grow, the exponential factor in the above equation is $-\omega^2\sigma_\tau^2 = -140$.

Shielded Bellows:

For the shielded bellows with $d = 5.5$ mm TBCI computes $k_{\parallel tot} = 0.010$ V/pC per shielded bellows. Inserting the SSC parameters into Eq. (15) yields 1.5 W of power lost in each shielding unit. Assuming the ring needs 4000 such units, the total power loss is 6 kW. This is quite a large value for the SSC.

The shielded bellows with $d = 4.0$ mm loses 0.9 W per shielding unit. For the shielded, shorted bellows with $d = 4.0$ mm the power loss again becomes negligible as in the simple bellows case. As we saw in the transverse case, shorting the shielded bellows pushes the first rise of $\Re e(Z_{\parallel})$ to higher frequencies. In the time domain we can say that with the shorting washer in place all the energy lost by the front half of the bunch is picked up by the back half. Without it, ten times as much energy is radiated by the head. In addition, most of the energy lost by the head is radiated between the two shielding tubes and doesn't return to the tail (See Fig. 7).

The lesson from these longitudinal computations is that if one wants to shield the bellows, then either the depth d must be made very small or the gap between the shielding tubes should be closed. Alternatively, one could design a shielding structure with only gradual discontinuities, such as those planned for LEP.[13] To conclude this section we summarize some key features of the bellows impedance calculations in Table 1.

Table 1. Bellows Contribution to the SSC Impedance and Power Loss

Bellows Type	$\Im m(Z_\perp(0))$	Power
simple bellows	-43.0 MΩ/m	0.0 kW
shielded ($d = 5.5$ mm)	-8.0 MΩ/m	6.0 kW
shielded ($d = 4.0$ mm)	-4.4 MΩ/m	3.6 kW
shorted ($d = 4.0$ mm)	-2.5 MΩ/m	0.0 kW

4. The Impedance of the Beam Position Monitors

There are many other contributions to the total impedance of the SSC vacuum chamber. One of the most important is the contribution from beam position monitors. The impedance of the position monitors has been discussed in Refs. 14 and 15; we quote the results here for completeness.

The BPM's discussed in Ref. 15 consist of 4 striplines positioned at 45° from the median plane so as not to intercept synchrotron radiation. The x or y position can be obtained by an appropriate linear combination of the signals from the 4 striplines. These would be placed at each quadrupole in the SSC.

The transverse impedance due to the stripline position monitors described above is given by

$$Z_\perp(\omega) = \frac{16PZ_pc\sin^2(\phi_0/2)}{\pi^2b^2\omega}[\sin^2(\omega\ell/c) + i\sin(\omega\ell/c)\cos(\omega\ell/c)] \tag{17}$$

where

$$P = 880 = \text{the number of pickups}$$

$$Z_p = 50\,\Omega = \text{pickup impedance}$$

$$b = 1.65\,\text{cm} = \text{ chamber radius}$$

$$\ell = 20\,\text{cm} = \text{length of pickup}$$

$$\phi_0 = 55^\circ \;\; = \text{angle subtended by one stripline}\ .$$

The impedance above is quite different from that due to the bellows. As with bellows the reactive part of the impedance below $\omega \approx 1/\sigma_\tau$ contributes to the frequency shift of mode 0. In addition, however, there is a sizable contribution from the resistive impedance at $\omega \approx 1/\sigma_\tau$ which contributes to the coupling of modes 0 and -1 and can lead to sizable growth rates. In all the calculations which follow the pickup impedance is included without modification.

5. Transverse Coherent Mode Coupling

In this section we show mode coupling due to the wake fields and impedances calculated in the previous sections. The theory of transverse mode coupling is discussed in Ref. 5 and more briefly in Ref. 6. The SSC parameters used in the calculation are given in Table 2, and the results for the various configurations are shown in Figs. 8 - 11. In each case the BPM impedance was included as well as the wake field from one of the various bellows schemes.

Table 2. SSC Parameters at Injection

Parameters	Notation	Values
Energy	E	1 TeV
Circumference	C	97.2 km
Chamber Radius	b	1.65 cm
Beta Function	β_{ave}	230 m
Energy Spread	σ_E	$1.5 \times 10^{-4} E$
Bunch Length	σ	7 cm
Freq. Slip Factor	η	1.8×10^{-4}
Synchrotron Tune	ν_s	6.0×10^{-3}
Protons per Bunch	N	1.45×10^{10}
Number of Bunches	n_b	9000

In Fig. 8 we show the results which include the BPM'S and simple bellows. Mode 0 moves linearly and collides with mode -1 at about $27\,\mu$A causing an instability. The threshold for this agrees quite well with the estimate given in Eq. (3). Notice also that the modes split apart again and re-stabilize and that modes -2 and -3 collide briefly to cause another 'bubble' of instability. The beam appears stable after $50\,\mu$A; however, this should *not* be taken seriously. In order to calculate the mode coupling accurately past $50\,\mu$A (in this case), it is necessary to include more modes. Roughly speaking, the highest mode which is included should be relatively unaffected if we are to believe the results of the calculation. However, in Fig. 8 we see that both -2 and -3 shift off the graph just past $50\,\mu$A. Thus, at least mode -4 and perhaps mode -5 must be included to calculate further. The growth rate of the instability is quite small ($\sim 0.04\nu_s$) which corresponds to an *e*-folding time of about 660 turns in the SSC.

The situation is somewhat different in the remaining figures. In Figs. 9 - 11 we show the case of BPM's plus each of the three schemes for shielding the bellows. In these cases the onset of the instability has been delayed and ranges from about $76\,\mu$A in Fig. 9 to about $123\,\mu$A in Fig. 11. Thus, the improvement in the threshold is a factor of 3 to 5. In addition, note that since the higher modes do not move, the calculation *can* be trusted out to the maximum current shown. The transverse mode coupling thresholds are summarized in Table 3 .

5.1 Fast Blow-up Thresholds

It is useful to calculate the threshold for fast blow-up for the case of the simple bellows. We must first assume that we believe the Q and thus the height of the peak in the impedance. If we use the peak value of the impedance at 13.5

Table 3. Transverse Mode Coupling Thresholds

Bellows Type	Threshold Current
simple bellows	$27\,\mu$A
shielded ($d = 5.5$ mm)	$76\,\mu$A
shielded ($d = 4.0$ mm)	$96\,\mu$A
shorted ($d = 4.0$ mm)	$123\,\mu$A

GHz and also include the small contribution of the pickups at that frequency, we find a 'threshold' of $40\,\mu$A. There is no fast blow-up below the threshold, but the actual instability may occur at somewhat larger currents. This indicates that we must be sure to include all the relevant higher modes when calculating transverse mode coupling threshold for currents higher that $40\,\mu$A. In particular, the stability in Fig. 8 above $50\,\mu$A is probably false.

On the other hand we can calculate the threshold for the shielded bellows as well. Here the situation is somewhat different in that the impedance does not have a peak at high frequency. In fact the fast blowup threshold is dominated by the impedance of the pickups at about 2 GHz and occurs at about $50\,\mu$A. This value is lower than the corresponding thresholds for transverse mode coupling; however, this does not indicate *another* instability. Since all the important modes are included for the shielded bellows, the transverse mode coupling threshold is correct. The 'fast blow-up' threshold is consistent with this in that the instability does occur at a larger current and has a rather large growth rate.

6. Feedback as a Cure for Transverse Mode Coupling

It has been shown in Refs. 6 and 16 - 18 that feedback can be used to increase the threshold of the transverse mode coupling instability. In addition there is recent experimental evidence to support this in the case of PEP.[19] For PEP it was found that both reactive feedback and resistive feedback increased the threshold by about a factor of 2. The theoretical prediction was that reactive feedback would increase the threshold significantly while resistive feedback would only increase it slightly.

The feedback used simply acts on the total dipole moment of the bunch. In the case of reactive feedback, a kick is supplied which shifts the coherent tune of the bunch while for resistive feedback the kick damps the dipole motion of the bunch. A simple damping of the dipole motion does not guarantee stability since there are higher modes which may be unstable. For the case of the SSC one would need a feedback system which acts on each bunch independently.

For the SSC we include feedback with sufficient power to shift the coherent tune by ν_s or to yield a damping rate of $i\nu_s$. The results are shown in Figs. 12 and 13 where we treat the case of the BPM's and simple bellows. As in Fig. 6, we cannot trust the results beyond about 0.05 mA since we have only included modes up to -3. However, it seems that both reactive and resistive feedback can increase the threshold by about a factor of 2.

7. Conclusions

In this paper we have presented the calculations of the wake fields and impedances for several different bellows schemes for the SSC and have shown how to scale the results to different designs. After including the additional impedance due to beam position monitors we have examined the transverse mode coupling instability. For the simple bellows we find a threshold for instability of about $26\,\mu$A for the single bunch current. The parameters for the SSC in Table 2 call for a single bunch current of $7.2\,\mu$A. Since there will be other sources of impedance, this is perhaps a bit too close.

We have studied two ways of raising the threshold. First we shielded the bellows with sliding contacts. This increases the threshold by a factor of 3 to 5 depending upon which scheme is used. In addition, we find that both reactive and resistive feedback increase the threshold by at least a factor of 2. Note that these values are for the representative simple and shielded bellows we have chosen for this study. The exact factors, however, will depend on the specific parameters of the bellows chosen.

Unfortunately, for the designs chosen to shield the bellows without a shorting washer, there are significant energy losses which would probably be unacceptable at cryogenic temperatures. However, if the shorted, shielded bellows design is impractical, it should be possible to decrease the losses for the unshorted case by an order of magnitude by decreasing the gap between the shielding tubes by this same factor.

8. Acknowledgements

We would like to thank Alex Chao, Albert Hofmann, Perry Wilson, and Bruno Zotter for useful discussions and Tor Raubenheimer for help with computations and figures.

REFERENCES

1. R. D. Ruth, Proc. of the Workshop on Acc. Physics Issues for the SSC, Ann Arbor, MI, p. 151 (1983) and LBL-17253 (1984).
2. H. Henke, LEP Note 454 (1983).
3. R. H. Siemann, private communication.
4. R. D. Ruth and J. M. Wang, IEEE Trans. Nucl. Sci., **NS-28**, No. 3, p. 2405 (1981).
5. R. D. Ruth, Brookhaven Formal Report BNL 51425 (1981).
6. R. D. Ruth, Proc. 12^{th} Int. Conf. on High Energy Acc., Fermilab, Batavia, IL, p. 389 (1983).
7. T. Weiland, DESY **82**-015 (1982) and Nucl. Instr. and Meth. **212**, 13 file (1983).
8. K. Bane and B. Zotter, Proceedings of the 11^{th} Int. Conf. on High Energy Accelerators, CERN (Birkhäuser Verlag, Basel,1980), p. 581.
9. R.K. Cooper, S. Krinsky and P.L. Morton, Particle Accel. **12**, 1 (1982).
10. See for example P. Wilson in *Physics of High Energy Particle Accelerators*, AIP Conf. Proc. No. 87, (Am. Inst. of Physics, New York, 1982), Sec. 11.1.

11. K.Y. Ng, Fermilab Report FN-389.

12. E. Keil, Nucl. Instr. and Meth., **100**, 419 (1972).

13. B. Zotter, private communication.

14. Robert E. Shafer, IEEE Trans. on Nucl. Sci., **NS-32**, No. 5, p. 1933 (1983).

15. R. E. Shafer, contribution to this workshop.

16. R. D. Ruth, CERN-LEP-TH/83-22 (1983).

17. S. Myers, LEP Note 498 (1983).

18. S. Myers, SLAC/AP-30,(1984).

19. M. Donald, A. Hofmann, T. Martin, P. Morton, S. Myers, J. M. Paterson, J.-L. Pellegrin, R. D. Ruth and P. Wilson, *Feedback Experiment at PEP*, to be submitted for publication.

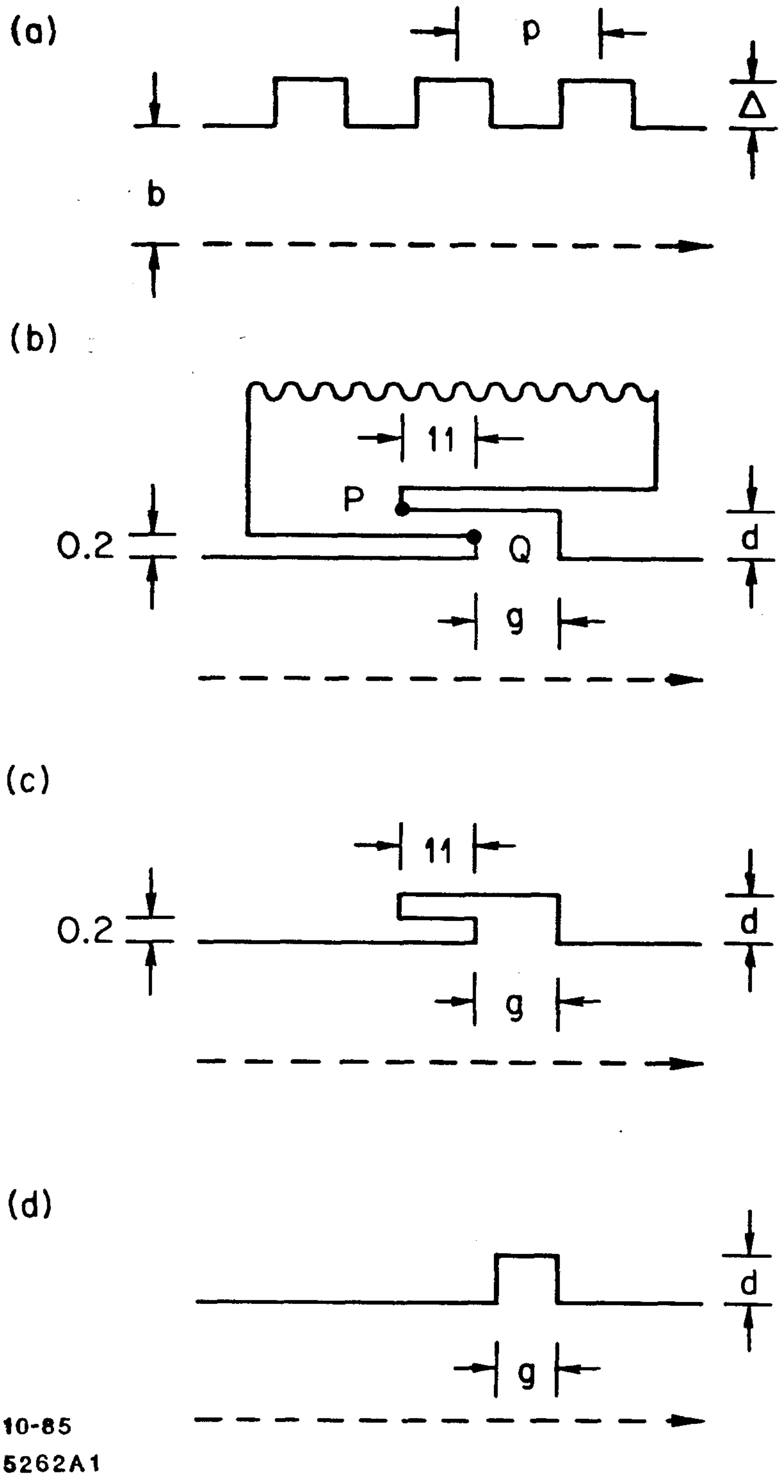

Fig. 1. Schematic Layout of the Bellows Schemes Studied. Dimensions Given are in Centimeters.

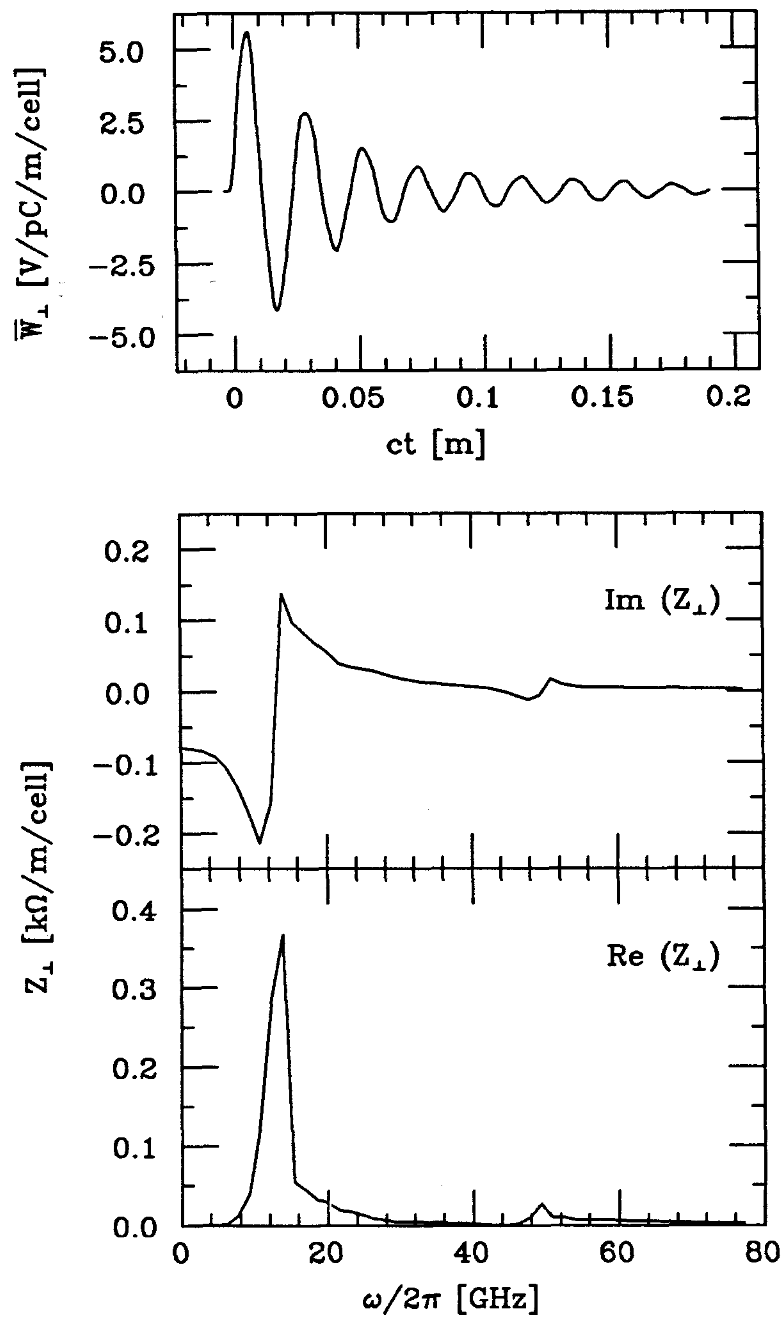

Fig. 2. Simple Bellows Wake Field and Impedance.

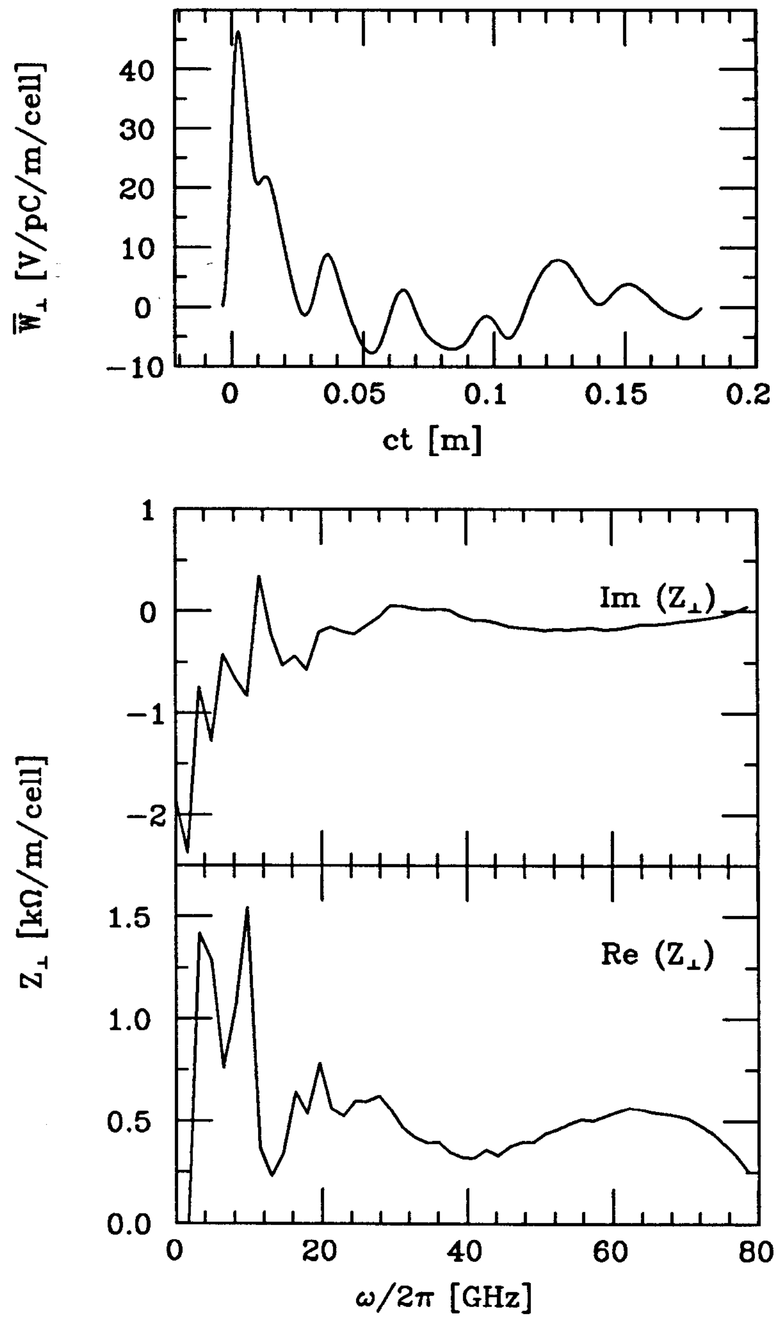

Fig. 3. Sliding Bellows Wake Field and Impedance.

(Depth d = 5.5 mm)

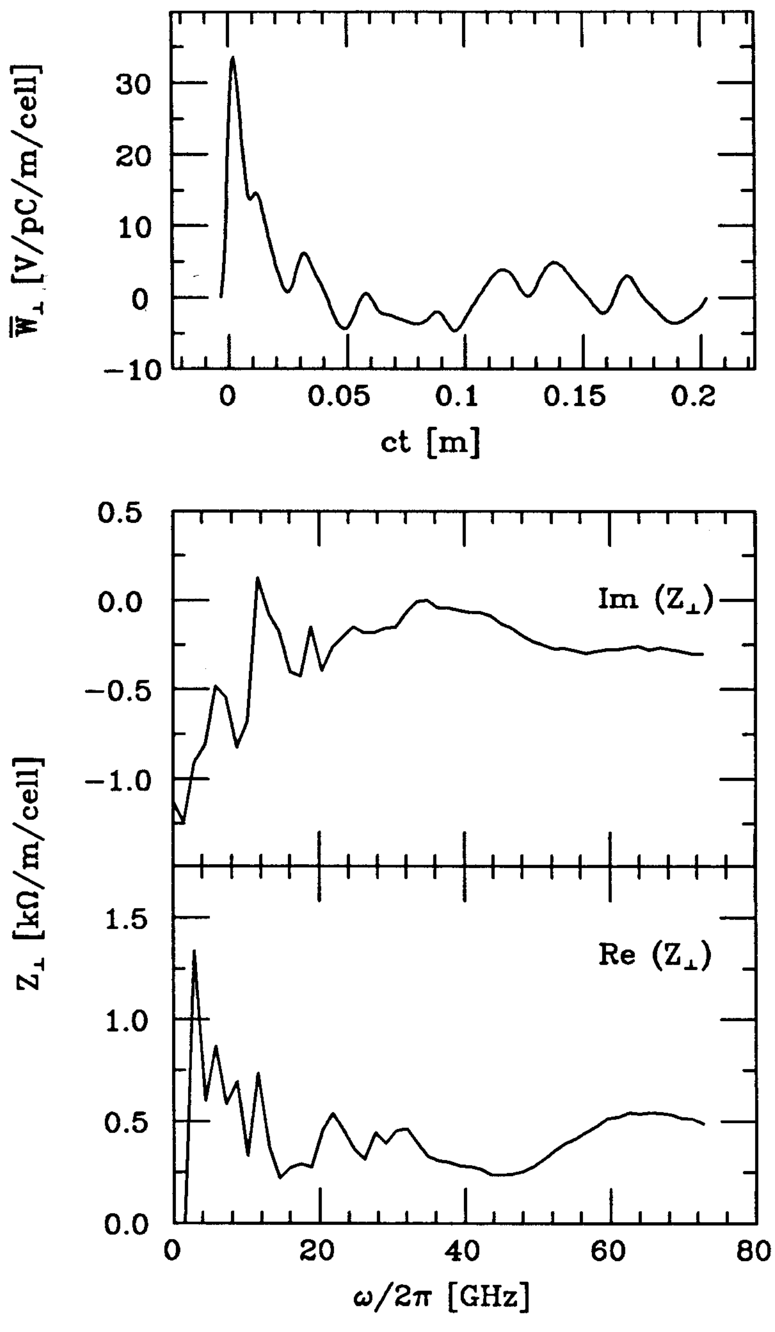

Fig. 4. Sliding Bellows Wake Field and Impedance.

(Depth d = 4.0 mm)

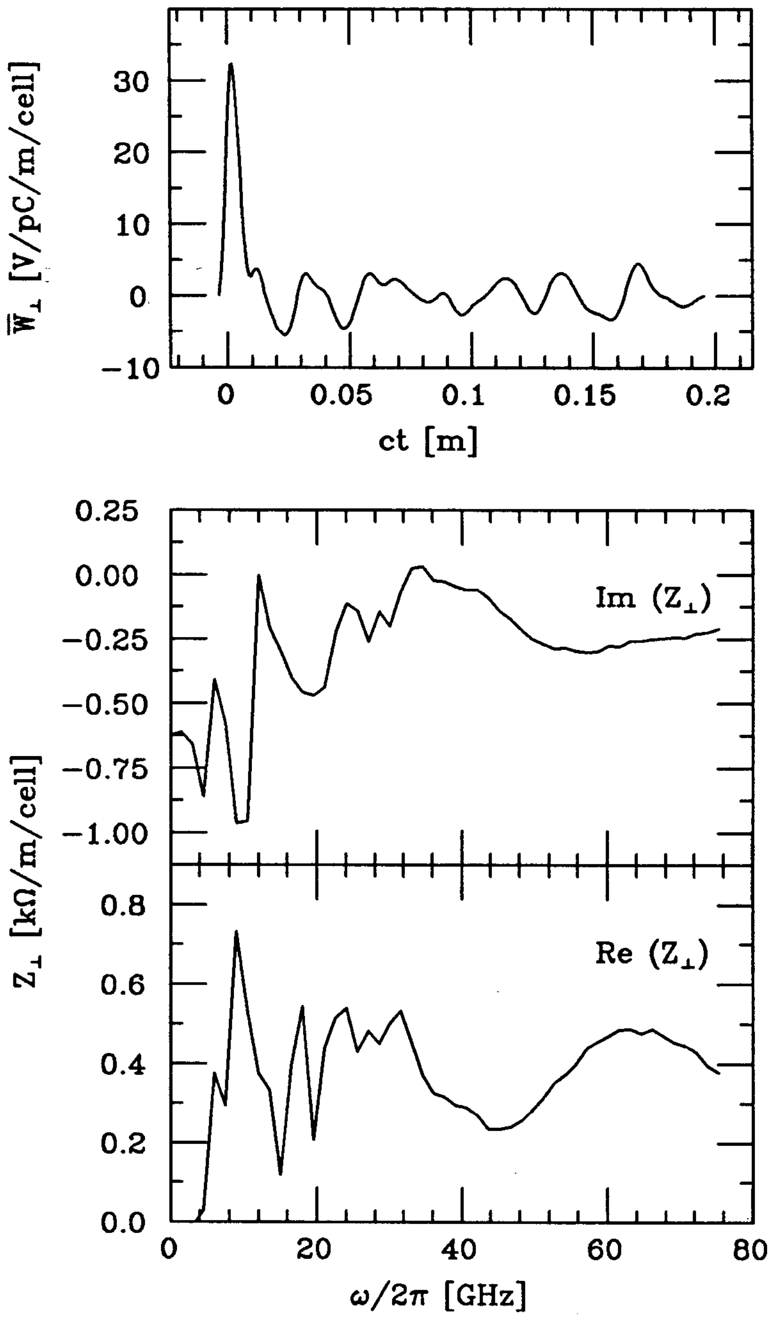

Fig. 5. Shorted Sliding Bellows Wake Field and Impedance.

(Depth d = 4.0 mm)

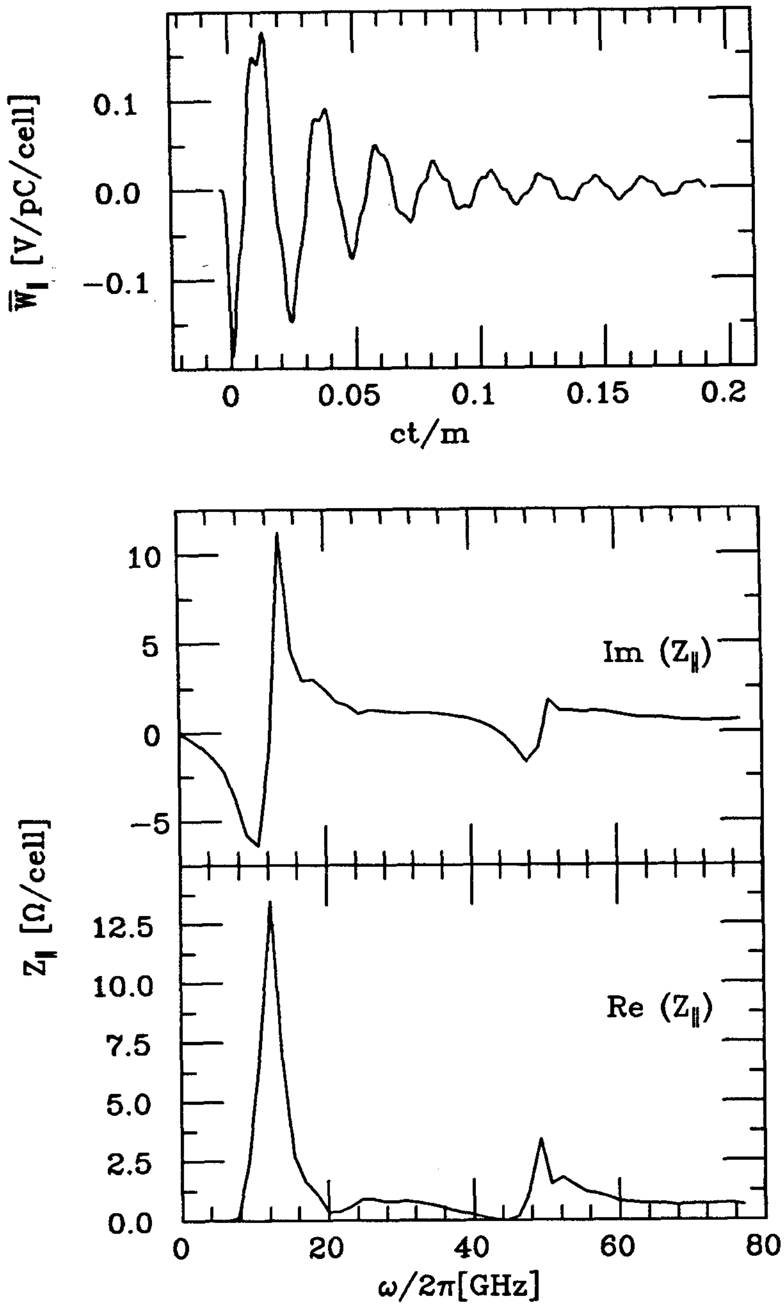

Fig. 6. Simple Bellows Longitudinal Wake Field and Impedance

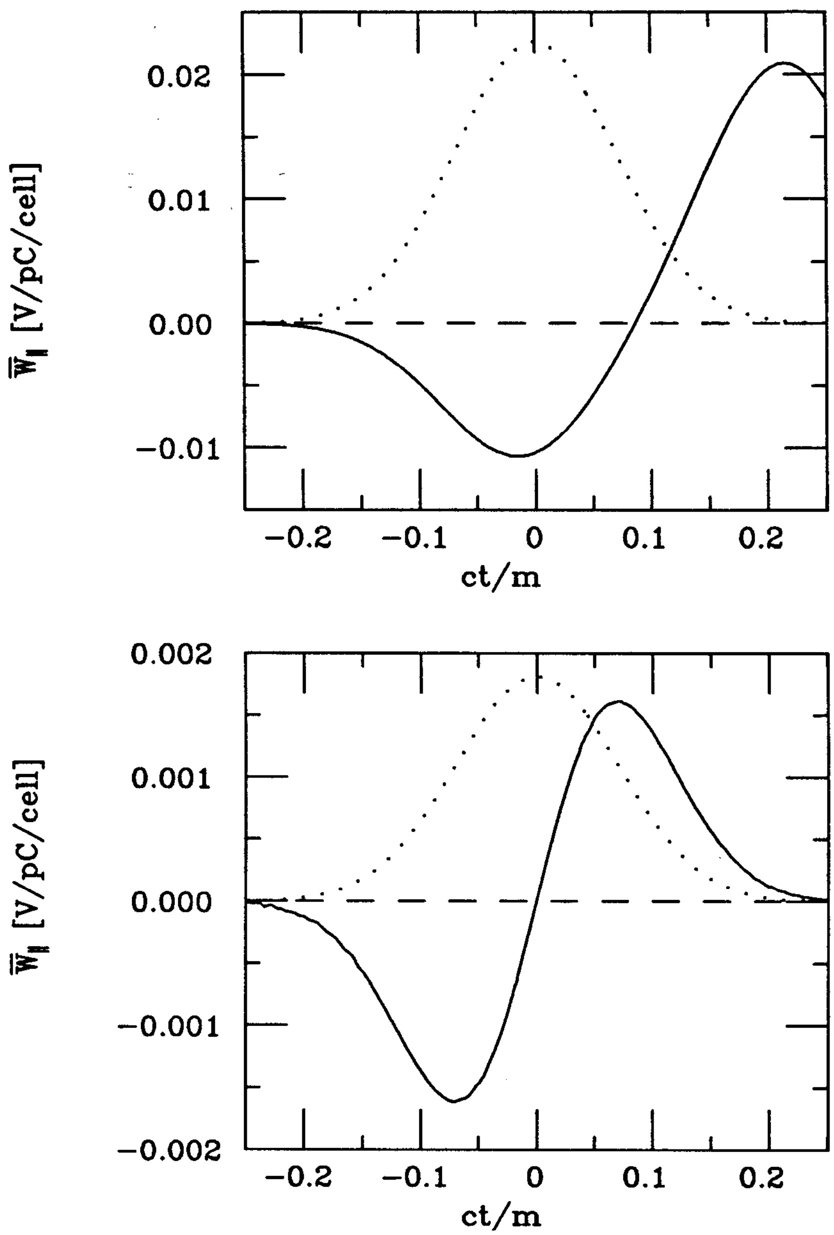

Fig. 7. Wake Field of Shielded (top) and Shielded, Shorted (bot) Bellows when $c\sigma_\tau$= 7cm. d= 4 mm. Dots Show the Bunch Shape with Head to the Left.

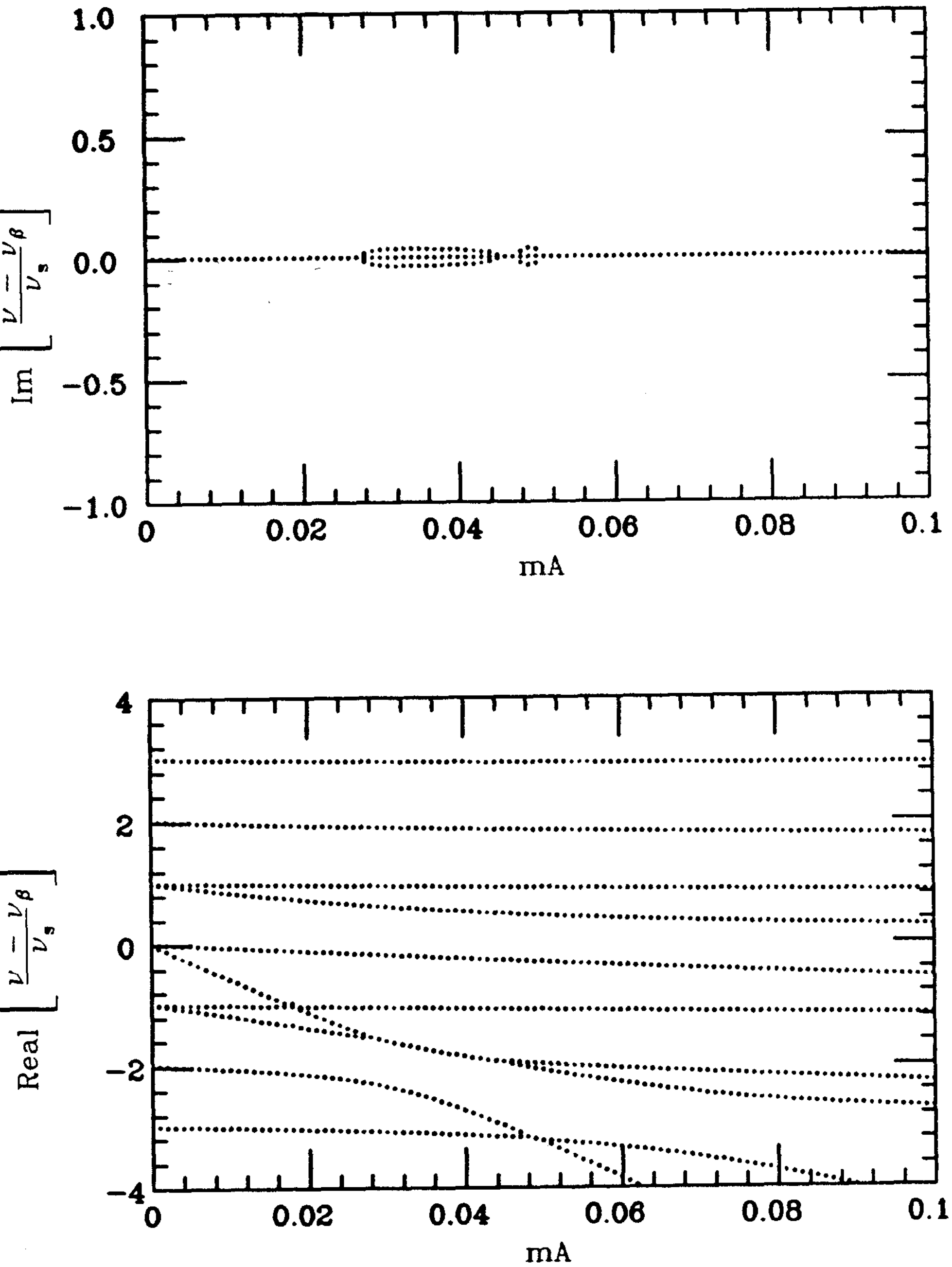

Fig. 8. Transverse Mode Coupling for the case including BPM's and simple bellows.

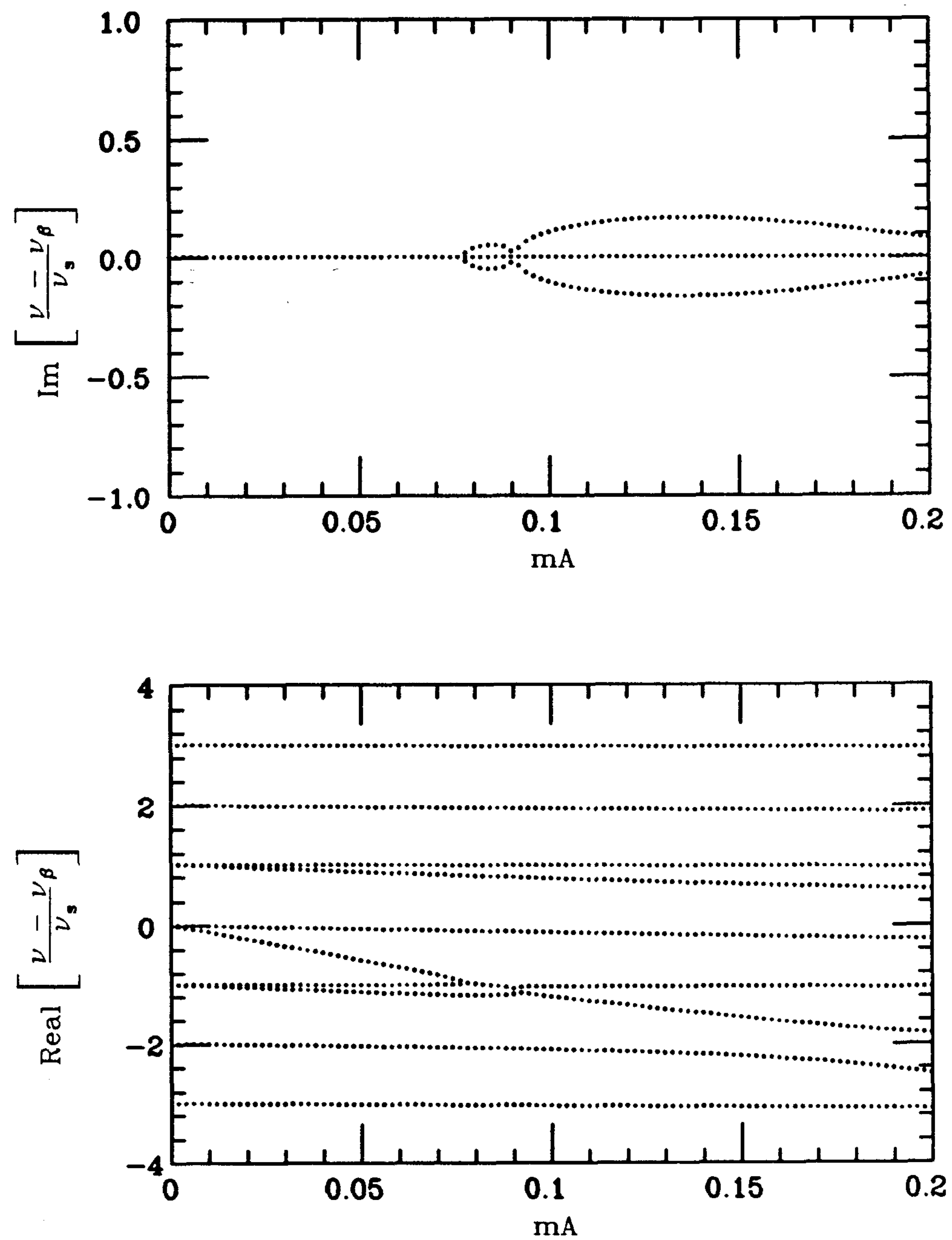

Fig. 9. Transverse Mode Coupling for the case including BPM's and shielded bellows (d = 5.5 mm).

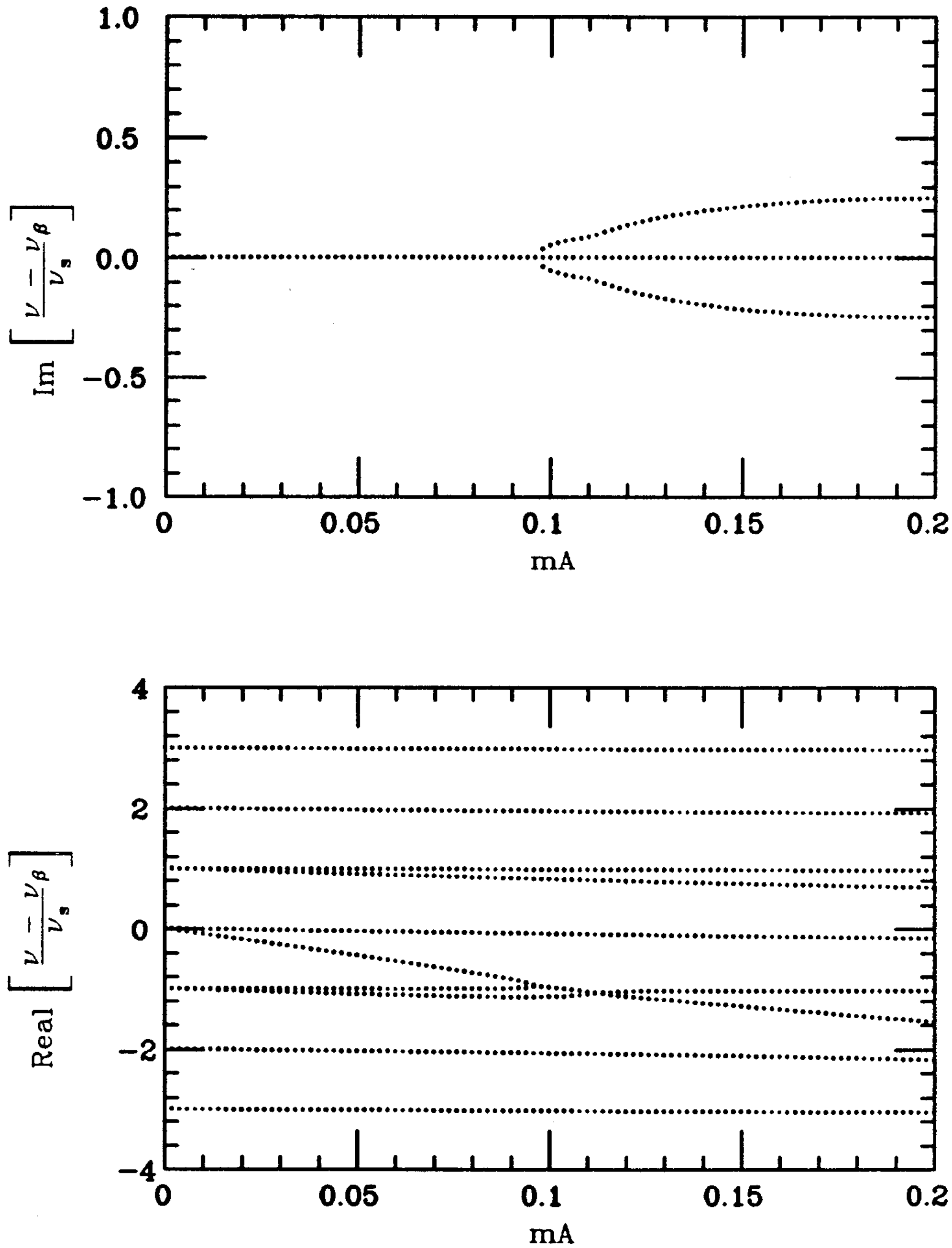

Fig. 10. Transverse Mode Coupling for the case including BPM's and shielded bellows (d = 4.0 mm).

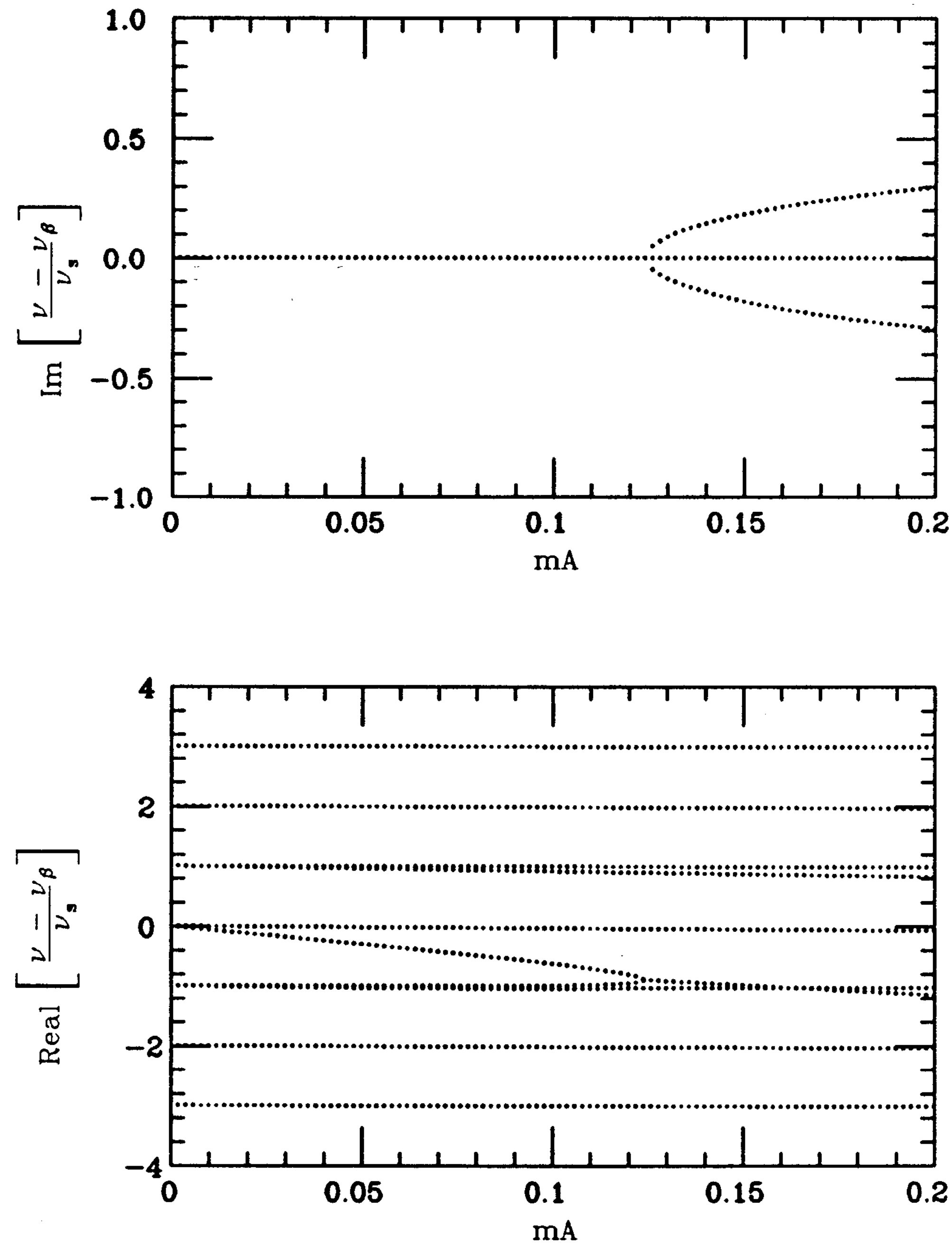

Fig. 11. Transverse Mode Coupling for the case including BPM's and shorted shielded bellows (d = 4.0 mm).

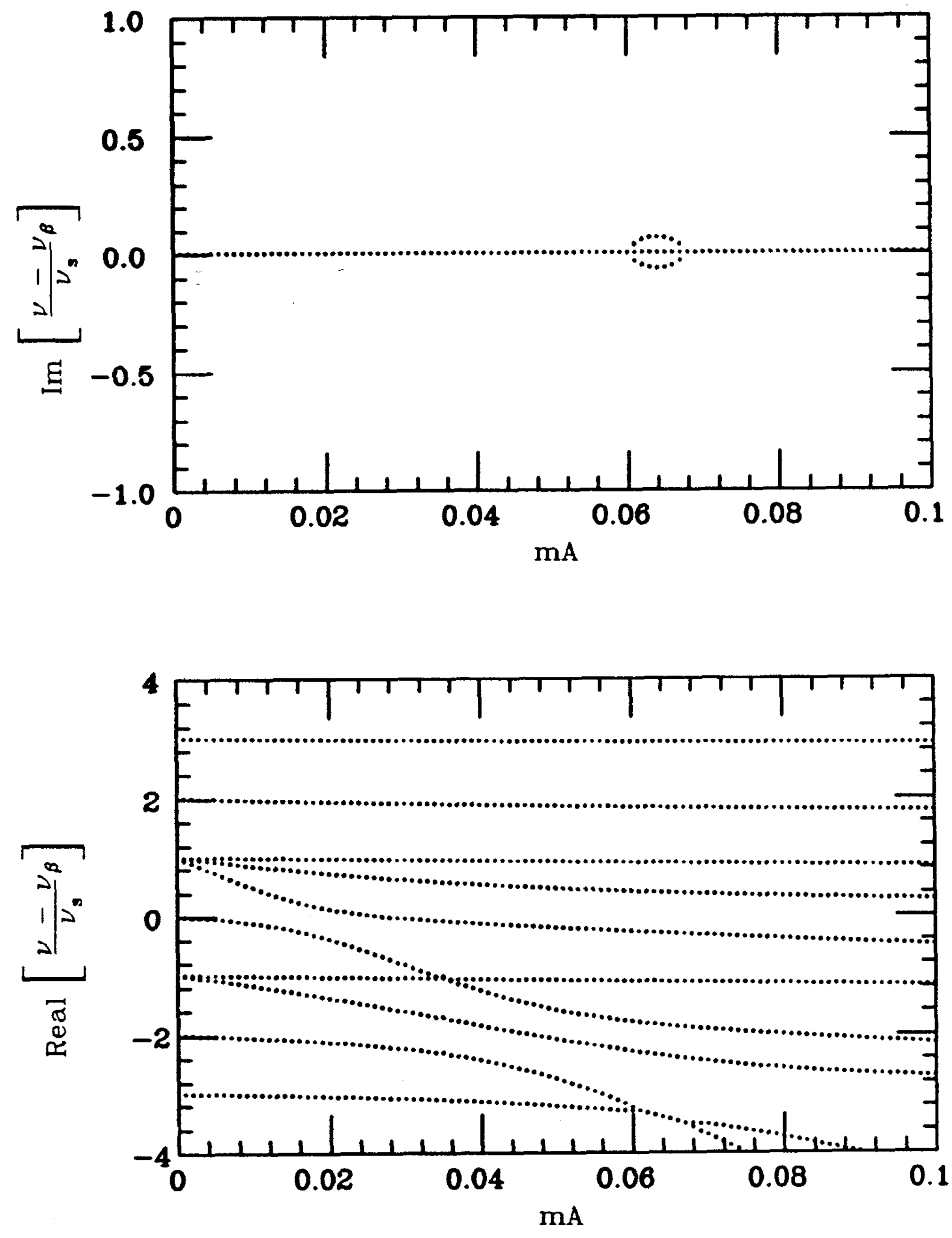

Fig. 12. Transverse Mode Coupling with Reactive Feedback ($\Delta\nu = \nu_s$) including BPM's and simple bellows.

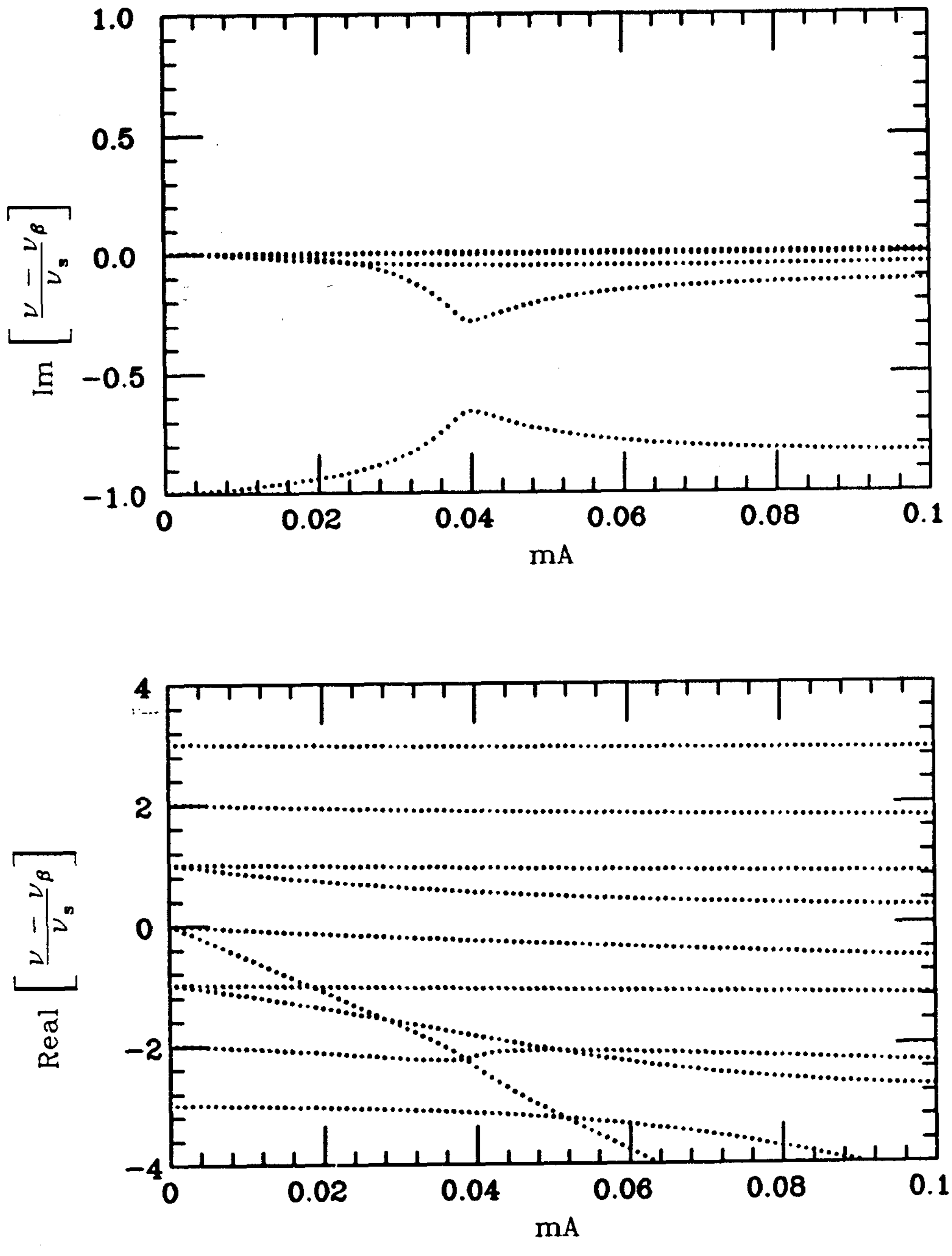

Fig. 13. Transverse Mode Coupling with Resistive Feedback ($\Delta\nu = -i\nu_s$) including BPM's and simple bellows.